9. Transfection of COS-1 or CV-1 cells (American Type Culture Collection) was done by calcium phosphate precipitation [F. L. Graham and A. J. van der Eb, *Virology* **52**, 456 (1973)]. At 48 hours after transfection, cells were metabolically labeled for 15 min at 37°C with [^{35}S]methionine (0.5 mCi/ml) (*5*). Labeled cells were removed from plates, solubilized in lysis buffer [0.5% (w/v) Triton X-100, 0.3 M NaCl, and 50 mM tris-HCl at pH 7.4], and centrifuged for 15 min at high speed. Supernatants were added to Abs bound to protein A–Sepharose beads. After incubation for 1 hour at 4°C, immunoprecipitates were washed five times with wash buffer [0.1% (w/v) Triton X-100, 0.3 M NaCl, and 50 mM tris-HCl at pH 7.4] and one time with phosphate-buffered saline (PBS). Samples were analyzed by SDS–polyacrylamide gel electrophoresis (PAGE) under reducing conditions on 13% acrylamide gels.
10. Immunoprecipitations were done with the following Abs: 10-2.16, a mouse monoclonal antibody (MAb) that binds both unassembled and assembled forms of A^k_β (*23*); FF282-4, a rabbit antiserum that reacts with the cytoplasmic tail of A^k_α, independent of assembly [A. J. Sant, L. R. Hendrix, J. E. Coligan, W. L. Maloy, R. N. Germain, *J. Exp. Med.* **174**, 799 (1991)]; 11-5.2, a mouse MAb to A^k_α associated with certain A^k_β haplotypes (*23*); and 40B, a mouse MAb that recognizes certain assembled $A_\alpha A_\beta$ heterodimers [M. Pierres, F. M. Kourilsky, J. P. Rebouah, M. Dossetto, D. Caillol, *Eur. J. Immunol.* **10**, 950 (1980)]. For simplicity and on the basis of their pattern of reactivity, Abs 10-2.16 and FF282-4 are referred to in the text as conformation independent, and 11-5.2 and 40B are referred to as conformation dependent. However, the actual nature of the epitopes recognized by these Abs is not known. Tac protein constructs were immunoprecipitated with 7G7, a mouse MAb to an extracellular epitope of the human Tac antigen [L. A. Rubin, C. C. Kurman, W. E. Biddison, N. D. Goldman, D. L. Nelson, *Hybridoma* **4**, 91 (1985)].
11. W. J. Leonard *et al.*, *Nature* **311**, 626 (1984).
12. Processing of newly synthesized αβ and αTα-βTβ complexes in CV-1 cells was analyzed by pulse-chase metabolic labeling and immunoprecipitation with the MAb to A^k_β (10-2.16). After 4 hours of chase, the amounts of α and αTα having one endoglycosidase H–resistant, *N*-linked oligosaccharide chain were 51 and 13%, respectively.
13. Most hydrophobic transmembrane sequences are thought to adopt an α-helical structure in lipid bilayers [D. M. Engelman, T. A. Steitz, A. Goldman, *Annu. Rev. Biophys. Biophys. Chem.* **15**, 321 (1986); S. J. Singer, *Annu. Rev. Cell Biol.* **6**, 247 (1990)]. Despite the demonstrated helix-breaking potential of Gly residues in water-soluble peptides [K. T. O'Neil and W. F. DeGrado, *Science* **250**, 646 (1990)], the presence of several Gly residues in transmembrane domains has been shown to be compatible with α-helical folding. For instance, transmembrane domains A and B of bacteriorhodopsin and ME of the *Rhodobacter sphaeroides* photosynthetic reaction center have four to five Gly residues and are known to be α helices by physical methods [R. Henderson *et al.*, *J. Mol. Biol.* **213**, 899 (1990); D. C. Rees, H. Komiya, T. O. Yeates, J. P. Allen, G. Feher, *Annu. Rev. Biochem.* **58**, 607 (1989)].
14. P. Cosson and J. S. Bonifacino, unpublished observations.
15. P. van den Elsen, B. A. Shepley, M. Cho, C. Terhorst, *Nature* **314**, 542 (1985).
16. Similar results were obtained by point mutation of Arg^{222} and Lys^{224} in β to Glu and Asp, respectively.
17. A probable arrangement of two interacting helices is a coiled-coil structure, in which the helices are wound around each other [G. E. Schulz and R. H. Schirmer, *Principles of Protein Structure* (Springer-Verlag, New York, 1979), pp. 79–81]. In such a structure, the potential strips of Gly residues would be tilted with respect to each other.
18. B.-J. Bormann, W. J. Knowles, V. T. Marchesi, *J. Biol. Chem.* **264**, 4033 (1989); M. A. Lemmon *et al.*, *ibid.* **267**, 7683 (1992).
19. L. K. Nielsen, J. D. Perera, L. F. Boyd, D. H. Margulies, J. McCluskey, *J. Immunol.* **144**, 2915 (1990); D. A. Wettstein, J. J. Boniface, P. A. Reay, H. Schild, M. M. Davis, *J. Exp. Med.* **174**, 219 (1991); L. J. Stern and D. C. Wiley, *Cell* **68**, 465 (1992).
20. G. A. Bishop, M. S. McMillan, G. Haughton, J. A. Frelinger, *Immunogenetics* **28**, 184 (1988).
21. P. Estess, A. B. Begovich, M. Koo, P. P. Jones, H. O. McDevitt, *Proc. Natl. Acad. Sci. U.S.A.* **83**, 3594 (1986).
22. Abbreviations for the amino acid residues are as follows: A, Ala; C, Cys; D, Asp; E, Glu; F, Phe; G, Gly; H, His; I, Ile; K, Lys; L, Leu; M, Met; N, Asn; P, Pro; Q, Gln; R, Arg; S, Ser; T, Thr; V, Val; W, Trip; and Y, Tyr.
23. V. T. Oi, P. P. Jones, J. W. Goding, L. A. Herzenberg, *Curr. Top. Microbiol. Immunol.* **81**, 115 (1978); N. S. Braunstein, R. N. Germain, K. Loney, N. Berkowitz, *J. Immunol.* **145**, 1635 (1990).
24. E. A. Kabat, in *Sequences of Proteins of Immunological Interest* (National Institutes of Health, Bethesda, MD, ed. 5, 1991), pp. 816–948.
25. Fixed or permeabilized cells were studied by immunofluorescence microscopy as described [J. S. Bonifacino, P. Cosson, N. Shah, R. D. Klausner, *EMBO J.* **10**, 2783 (1991)]. Nonpermeabilized cells were incubated for 1 hour at 4°C with culture medium containing MAb 10-2.16, followed by a 1-hour incubation at 4°C with a rhodamine-conjugated Ab to mouse immunoglobulins (1:200 dilution). Cells were then fixed with 2% formaldehyde and prepared for fluorescence microscopy.
26. We thank R. Klausner, R. Germain, D. Engelman, M. Lemmon, G. Storz, J. Humphrey, and M. Toledano for discussions and comments on the manuscript, and R. Germain, J. Salamero, and E. Long for gifts of reagents. Supported by a fellowship from the European Molecular Biology Organization (to P.C.).

26 May 1992; accepted 7 August 1992

Phase Coupling by Synaptic Spread in Chains of Coupled Neuronal Oscillators

Thelma L. Williams

Many neural systems behave as arrays of coupled oscillators, with characteristic phase coupling. For example, the rhythmic activation patterns giving rise to swimming in fish are characterized by a rostral-to-caudal phase delay in ventral root activity that is independent of the cycle duration. This produces a traveling wave of curvature along the body of the animal with a wavelength approximately equal to the body length. Here a simple mechanism for phase coupling in chains of equally activated oscillators is postulated: the synapses between the cells making up a "unit oscillator" are simply repeated in neighboring segments, with a reduced synaptic strength. If such coupling is asymmetric in the rostral and caudal directions, traveling waves of activity are produced. The intersegmental phase lag that develops is independent of the coupling strength over at least a tenfold range. Furthermore, for the unit oscillator believed to underlie central pattern generation in the lamprey spinal cord, such coupling can result in a phase lag that is independent of frequency.

An important feature of the neural activity that gives rise to locomotion in the lamprey is a rostral-to-caudal intersegmental delay that scales with the cycle duration, remaining equal to approximately 1% of the cycle per spinal cord segment at all swimming frequencies (*1*) (Fig. 1, a and b). Synaptic or conduction delays do not scale in this way, so the intersegmental timing must result from more complex interactions in the neural system. Although the mathematical analysis of the central pattern generator as a chain of coupled nonlinear oscillators (*2*) (Fig. 1c) has successfully predicted some unexpected behavior of the in vitro preparation of the lamprey (*3*), it gives no indication of what sort of neuronal interactions could mediate the coupling. It has been postulated (*4*) that the intersegmental phase lag in the lamprey is due to increased excitability of the most rostral segment, but experimental evidence indicates no such excitation in the lamprey (*5*). Buchanan (*6*) has shown by computer simulation that synaptic contacts between simulated unit oscillators can give rise to appropriate phase lags. In this report I suggest a form of intersegmental coupling with a simple, biologically plausible developmental rule: whatever synaptic contacts each neuron makes in its own segment, it must also make in neighboring segments but with a smaller synaptic strength. I will show by computer simulation that, with such "synaptic spread" between equally activated oscillators, a constant intersegmental phase lag can result as long as the connections between oscillators are asymmetric.

The detailed structure of the segmental oscillators in the lamprey is not known. However, a small network model (Fig. 1d) consisting of identified neurons that are rhythmically active during "fictive locomotion" (*7*) (neural activity with the same patterns as those recorded during locomotion) has produced oscillations with phase relations among the three cell types that are

Physiology Department, St. George's Hospital Medical School, University of London, London SW17 0RE, United Kingdom.

similar to those seen in the lamprey spinal cord in vitro (8).

The phase relations among E (excitatory), C (crossed inhibitory), and L (lateral inhibitory) cells in a unit oscillator in a connectionist simulation (6) (Fig. 2a) are similar to those observed in more elaborate biophysical simulations (9) and in the lamprey, but the number of adjustable parameters is an order of magnitude lower in the connectionist simulations (*10*). Because the values of such parameters are generally unknown, connectionist models have been used in the present study to keep the number of parameters to a minimum. The connectionist model is based on standard principles of synaptic current flow and membrane potential control, but action potentials are not simulated. Instead, the height of a cell's membrane potential above threshold is taken as a measure of the firing rate of the cell, and the conductance change in a postsynaptic cell is proportional to this firing rate (*11*).

When two equally activated oscillators are coupled by synaptic spread in one direction (Fig. 1e), they develop a phase relation in which the sending oscillator neither speeds up nor slows down the receiving oscillator (Fig. 2a). For this particular species of unit oscillator, a phase lag develops in which the segment receiving the coupling signals leads. Thus caudal-to-rostral coupling gives rise to a rostral-to-caudal delay. (If the two oscillators are given unequal activation, corresponding to unequal intrinsic frequencies, a different phase lag develops.) This phase lag remains approximately constant over the nearly fourfold range of cycle durations obtainable with this oscillator (Fig. 2b) and over a 16-fold range of intersegmental synaptic strengths (Fig. 2c).

A chain of such oscillators with coupling in only one direction shows a uniform intersegmental phase lag equal to that in Fig. 2a. There is much evidence in the lamprey, however, that intersegmental coupling is both rostral and caudal (*12*). If the synaptic spread is in both directions with equal strength, then a symmetric pattern results in which the leading oscillator is in the center of the chain and waves of activation travel toward both ends. This behavior is consistent with the mathematical analysis of coupled oscillators (*13*) but is not biologically realistic.

If, however, the intersegmental coupling is of unequal strength in the two directions, the resulting phase lag is uniform along all but a few segments on one end of the chain and is equal to what would occur if only the stronger coupling existed (*13*). In the simulations of Fig. 2, d and e, the synaptic strength of all connections from cells in one oscillator to cells in its

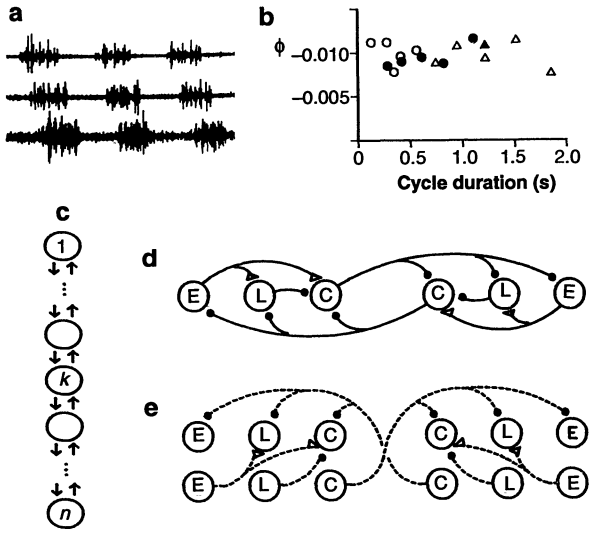

Fig. 1. The lamprey spinal cord as a chain of coupled oscillators. (**a**) Electromyographic activity recorded from an intact swimming lamprey (*15*), from ipsilateral myotomes separated by approximately 20 segments. The rhythmic pattern, which can also be produced by the spinal cord in vitro, consists of activity exhibiting a rostral-to-caudal delay and strict left-right alternation (not shown). (**b**) Independence of rostral-to-caudal phase timing on cycle duration. Phase lag (ϕ) calculated as time delay between burst activity in two ventral roots, divided by the cycle period and the number of segments separating the electrodes. Negative values represent rostral-to-caudal delay, consistent with the convention used in mathematical analysis (*2*). Filled circles, intact swimming lampreys; open circles, swimming lampreys with spinal cord transected just behind the gills; filled triangle, spontaneous activity, in vitro spinal cord; open triangles, activity induced by D-glutamate, in vitro spinal cord; data from Wallén and Williams (*15*). (**c**) Chain of oscillators with nearest neighbor coupling. An oscillator within the chain (*k*) receives both ascending and descending coupling signals, whereas the most rostral (1) or most caudal (*n*) oscillator receives coupling from one direction only. This produces a boundary layer (Fig. 2e) at the end that receives the dominant coupling (*13*). (**d**) Circuit postulated as the segmental oscillator in the lamprey (*7*), composed of identified neurons (*16*): crossed-caudal interneurons (C), lateral interneurons (L), and excitatory interneurons (E) (*7*). (**e**) Two oscillators coupled by caudal-to-rostral synaptic spread (synaptic connections within each unit not shown).

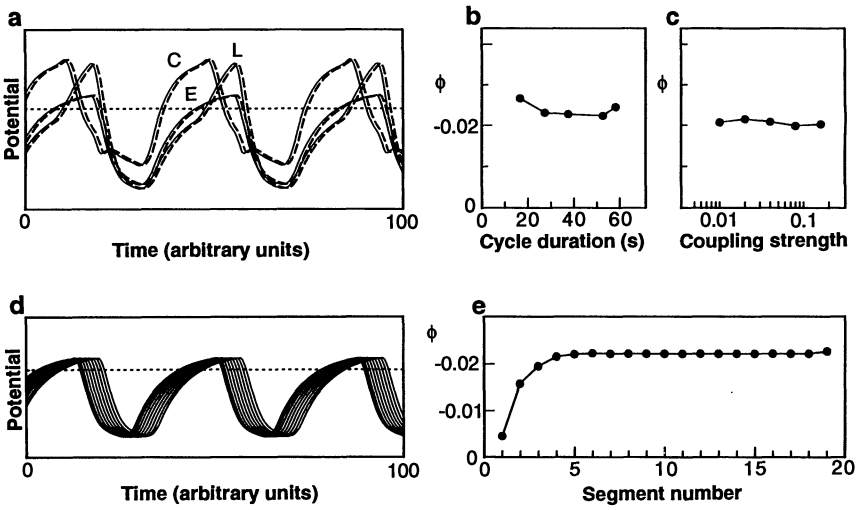

Fig. 2. Phase coupling between equally activated unit oscillators in simulations of the lamprey central pattern generator. (**a**) Time course of simulated membrane potential trajectories of the cells of Fig. 1e. Solid lines, rostral (receiving) segment; dashed lines, caudal (sending) segment; horizontal dotted line, action potential threshold. (**b**) Phase lag, measured between threshold crossings in ipsilateral C cells, changed little with cycle duration. Frequency was raised by an increase in the tonic drive to E cells only (*6*). The magnitude of ϕ depended somewhat on the particular choice of parameters used in simulating a single oscillator, varying between approximately −0.005 and −0.04 over the parameter space explored in this study that supported oscillations. (**c**) Independence of ϕ on intersegmental coupling strength (the fraction of synaptic strength in a unit oscillator). (**d**) Simulated membrane potentials of ipsilateral E cells of the first 10 of a chain of 20 oscillators. Consecutive potential records are from segments 1 to 10 in order (that is, activation travels rostral to caudal). Ascending coupling strength, 0.05; descending coupling strength, 0.02. (**e**) Phase lags calculated between E cells in this simulation. The smaller ϕs at the rostral end in (d) are seen here as a narrow boundary layer (a few segments). For simulations of longer chains with the same coupling, the boundary layer remains the same length (and hence a smaller fraction of the length of the chain).

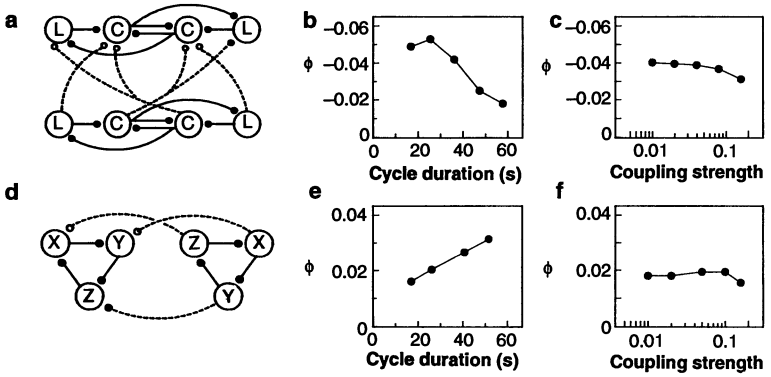

Fig. 3. (**a**) A pair of four-cell oscillators coupled by caudal-to-rostral synaptic spread. (**b**) Dependence of ϕ on cycle duration. (**c**) Dependence of ϕ on coupling strength. (**d**) A pair of three-cell oscillators (*14*) coupled by ascending synaptic spread. Cells represented by X, Y, and Z are identical; phase delays measured between analogous cells (X_1 and X_2). (**e** and **f**) Dependence of ϕ on cycle duration and coupling strength, respectively. The negative values of ϕ in (b) and (c) represent a rostral-to-caudal traveling wave; the positive values in (e) and (f) represent a caudal-to-rostral wave.

rostral neighbor were 0.05 times the strength of the synapses within the oscillator, whereas all the synapses in the caudal direction were 0.02 times the intrasegmental strength. Except for a small boundary layer near the rostral end, the intersegmental phase lag was uniform along the cord (Fig. 2, d and e) and was approximately equal to the lag shown in Fig. 2a, where only ascending coupling was present. As long as the descending coupling was weaker than the ascending coupling, its only effect was to produce a boundary layer at the rostral end; if it was greater in strength than the ascending coupling, the phase lag was positive (the wave traveled caudal to rostral) and the boundary layer was at the caudal end. The phase lag was relatively independent of the strength of the dominant coupling (Fig. 2c).

The phase lag was also independent of oscillator frequency (Fig. 2b) if this rate was raised by an increase in the tonic excitatory drive to the E cells alone. If the frequency was raised by an increase in the tonic drive to all cells in the circuit, the phase lag increased in magnitude with increasing cycle duration.

To investigate the general effect of synaptic spread, I simulated chains consisting of even simpler unit oscillators. An oscillator is shown in Fig. 3a with the same connectivity as before (Fig. 1d) but without the excitatory cells. The phase lag that developed when such oscillators were coupled by synaptic spread was not independent of frequency (Fig. 3b), whether frequency was controlled by a change in tonic drive to all cells equally or to one cell type alone. It was possible to maintain a constant phase lag over a range of frequencies by a change in the ratio of C to L activation for each frequency, but small alterations in this ratio produced significant changes in phase lag, which is not biologically realistic. An oscillator consisting of only three inhibitory neurons in a ring (*14*) (Fig. 3d) also demonstrated a phase lag when coupled by synaptic spread, but the lag was positive rather than negative: the oscillator sending the coupling leads (Figs. 3, e and f). Thus, in a chain of these oscillators, the wave of activity would travel in the same direction as the dominant coupling, unlike the dynamics in the oscillators of Figs. 1d and 3a.

All the phase lags that emerged in this study were a few percent of the cycle duration, which is near synchrony. This tendency of equal oscillators coupled by synaptic spread to synchronize is intuitively reasonable because the coupling is a repeat of the connections that give rise to the rhythmicity of the unit oscillator. However, if at synchrony the coupling tends to speed up or slow down the receiving oscillator, then a phase lag develops. In general, the faster oscillator leads, so if the coupling at synchrony increases the frequency of the receiving oscillator, a negative phase lag develops when ascending coupling is dominant; if coupling decreases the frequency, then a positive phase lag develops.

For the three-cell oscillator, increasing the synaptic strengths in a unit network decreases the frequency of its oscillations. If two coupled oscillators are synchronous, the effect of the sending oscillator is equivalent to increasing the synaptic strengths in the receiving oscillator, which slows that oscillator down. Thus ascending synaptic spread gives rise to a positive phase lag in this network. In the four- and six-cell networks, an increase in the synaptic strengths from the L cells increases unit oscillator frequency, but an increase from the C cells decreases it. The negative phase lag that develops indicates that coupling at synchrony leads to an overall acceleration in frequency. Hence, domination of the network by the L cells could account for the rostral-to-caudal phase lag that develops between equally activated oscillators.

The constancy of phase lag with oscillator frequency in the six-cell network when frequency is controlled by the E cells (Fig. 2b) indicates that an appropriate balance between the acceleratory and deceleratory effects of coupling is maintained at all cycle durations. This seems to be the feature required to maintain a phase lag independent of frequency, such as in the lamprey.

Synaptic spread produced a nonzero phase lag (albeit only a few percent of the cycle) for all of these oscillators. For any form of coupling that results in zero phase lag (synchrony), a traveling wave of activation requires that the oscillator on one end of the chain be given a different level of activation than the rest of the chain. Because there is no evidence of this in the lamprey, such coupling seems unlikely.

Stable phase timing between neural oscillators may thus occur in response to the same synaptic connections as those within a unit oscillator, and the characteristic phase lag depends only on the nature of the oscillators rather than on the strength of the coupling, as long as it remains asymmetric. Furthermore, with some networks such phase coupling may be independent of cycle duration, as in the lamprey central pattern generator.

REFERENCES AND NOTES

1. The lamprey spinal cord has approximately 100 segments, so there is about one wavelength of activation on the body at all times, leading to approximately one wavelength of curvature. Maintaining this whole number of wavelengths at all swimming speeds is important for minimizing lateral thrust [reviewed in K. A. Sigvardt, *Amer. Zool.* **29**, 19 (1989)]. Grillner first showed that phase lag is independent of frequency in the dogfish [S. Grillner, *Exp. Brain Res.* **20**, 459 (1974)] and it was subsequently shown for the eel [S. Grillner and S. Kashin, in *Neural Control of Locomotion*, R. M. Herman, S. Grillner, P. S. G. Stein, D. G. Stuart, Eds. (Plenum, New York, 1976), p. 181], lamprey [A. H. Cohen and P. Wallen, *Exp. Brain Res.* **41**, 11 (1980)], and trout [T. L. Williams *et al.*, *J. Exp. Biol.* **143**, 559 (1989)].
2. A model for the lamprey spinal central pattern generator as a chain of coupled oscillators was proposed by A. H. Cohen, P. J. Holmes, and R. H. Rand [*J. Math. Biol.* **13**, 345 (1982)], in which a greater intrinsic frequency at the rostral end of the chain gave rise to a uniform phase lag along the cord. Subsequent experiments by Cohen (*5*) failed to reveal a gradient of intrinsic frequencies in small pieces of spinal cord. Subsequently, a general mathematical analysis of coupled chains of oscillators showed that uniform phase lags can be produced without a gradient of frequencies, if certain assumptions are made about the coupling between adjacent oscillators and if the coupling is asymmetric in the rostral and caudal directions [G. B. Ermentrout and N. Kopell, *SIAM J. Math. Anal.* **15**, 215 (1984); *J. Math. Biol.* **29**, 155 (1991); N. Kopell and G. B. Ermentrout, *Math. Biosci.* **90**, 87 (1988)].
3. N. Kopell, G. B. Ermentrout, and T. L. Williams [*SIAM J. Appl. Math.* **51**, 1397 (1991)] predicted

that the frequency ranges over which fictive locomotion could be entrained by applied movement to the rostral and to the caudal ends should be unequal and that the resting frequency should provide a limit for entrainment for one end but not the other. These nonintuitive predictions were confirmed by experiment [T. L. Williams, K. A. Sigvardt, N. Kopell, G. B. Ermentrout, M. P. Remler, *J. Neurophysiol.* **64**, 862 (1990)]. Furthermore, N. Kopell and G. B. Ermentrout [*SIAM J. Appl. Math.* **50**, 1014 (1990)] predicted a specific pattern of changes in phase lag when different portions of an in vitro preparation are bathed in different amino acid concentrations. These predictions were confirmed experimentally [(K. A. Sigvardt, N. Kopell, G. B. Ermentrout, M. P. Remler, *Soc. Neurosci. Abstr.* **17**, 122 (1991)]. Similar results were obtained by Matsushima and Grillner (*4*), but these authors placed a different interpretation on the data.

4. T. Matsushima and S. Grillner, *J. Neurophysiol.* **67**, 373 (1992).
5. A. H. Cohen, *J. Neurosci. Methods* **21**, 113 (1987).
6. J. T. Buchanan, *Biol. Cybern.* **66**, 367 (1992).
7. _____ and S. Grillner, *Science* **236**, 312 (1987).
8. S. Grillner, J. T. Buchanan, A. Lansner, *Neurosci. Lett.* **89**, 31 (1988).
9. O. Ekeberg *et al.*, *Biol. Cybern.* **65**, 81 (1991); P. Wallén *et al.*, *J. Neurophysiol.*, in press.
10. For a review of modeling the central pattern generator for locomotion in the lamprey, see K. Sigvardt and T. L. Williams [*Semin. Neurosci.* **4** (no. 1), 37 (1992)].
11. Each cell in a simulation has an "activation" variable a_i, which represents its membrane potential trajectory. If a_i is above a threshold value th_i, it is taken as a measure of the firing rate f_i of the cell, with $f_i = 0$ when $a_i < th_i$ and $f_i = a_i - th_i$ when $a \geq th_i$. In each time step, the activation variable of cell i will change as a result of synaptic input or decay, as given by:

$$\Delta a_i = e_i(v_{ie} - a_i) + \tau_i(r_i - a_i) + \Sigma_j w_{ij} f(v_{ij} - a_i)$$

where e_i is the tonic excitatory drive to cell i, v_{ie} represents the "reversal potential" for the excitatory drive, r_i represents the resting potential, τ_i is a time constant for return to r_i, w_{ij} represents the weight of the synapse from cell j to cell i, and v_{ij} represents the "reversal potential" for the synapse from cell j to cell i.

Normalized values were used for all the parameters: $e_i = 0.1$ for C cells, 0.01 for L cells, and 0.025 for E cells; for all cells: $v_{ie} = 1.0$, $th_i = 0$, $\tau_i = 0.1$, and $r_i = 0$; $w_{ij} = 1.0$ for all synapses; $v_{ij} = 1.0$ for all excitatory synapses and -1.0 for all inhibitory synapses.

12. C. M. Rovainen, *J. Comp. Neurol.* **154**, 189 (1974); *J. Neurophysiol.* **54**, 959 (1989); J. T. Buchanan, *ibid.* **47**, 961 (1982); N. Dale, *J. Neurosci.* **6**, 2662 (1986).
13. N. Kopell and G. B. Ermentrout, *Commun. Pure Appl. Math.* **39**, 623 (1986); T. L. Williams, *Neural Comput.* **4**, 546 (1992).
14. Z. Szekely, *Acta Physiol. Acad. Sci. Hung.* **27**, 285 (1965).
15. P. Wallén and T. L. Williams, *J. Physiol. (London)* **347**, 225 (1984).
16. J. T. Buchanan and A. H. Cohen, *J. Neurophysiol.* **47**, 948 (1982).
17. I thank G. Bowtell for writing software and K. Sigvardt for valuable comments on the manuscript. Supported by the Science and Engineering Research Council (U.K.).

13 April 1992; accepted 9 July 1992

Burst Firing in Dopamine Neurons Induced by *N*-Methyl-D-Aspartate: Role of Electrogenic Sodium Pump

Steven W. Johnson, Vincent Seutin, R. Alan North

Dopamine-containing neurons of the mammalian midbrain are required for normal behavior and movements. In vivo they fire action potentials in bursts, but in vitro they discharge regularly spaced action potentials. Burst firing in vitro has now been shown to be robustly induced by the glutamate agonist *N*-methyl-D-aspartate (NMDA) although not by the non-NMDA agonists kainate or quisqualate. The hyperpolarization between bursts of action potentials results from electrogenic sodium ion extrusion by a ouabain-sensitive pump. This mechanism of burst generation in mammalian neurons may be important in the pathophysiology of schizophrenia and Parkinson's disease.

The dopamine-containing neurons of the ventral midbrain project predominantly to the prefrontal cortex, nucleus accumbens, and striatum and are involved in the control of affect, movement, and drug-seeking behavior (*1*). In freely moving rats, they discharge with single spikes or with bursts of spikes (*2*). The bursts are not seen in vitro (*3–8*), perhaps because of the loss of critical afferent inputs (*4*, *5*) that release excitatory amino acids (*9*, *10*). We tested this hypothesis by applying excitatory amino acids while recording from the cells in vitro (*6*, *7*, *11*).

Vollum Institute and Department of Neurology, Oregon Health Sciences University, Portland, OR 97201

N-Methyl-D-aspartate (NMDA) (10 to 30 μM) changed the firing pattern from regularly spaced single spikes to one in which bursts of two to ten action potentials were separated by large hyperpolarizations (up to 40 mV) lasting 1 to 5 s (Fig. 1A). The action of NMDA continued throughout its application (up to 8 hours), reversed quickly on washing, and was antagonized by the NMDA receptor blocker D,L-2-amino-5-phosphonopentanoic acid (APV) although not by 6-cyano-2,3-dihydroxy-7-nitro-quinoxaline (CNQX), which blocks non-NMDA receptors (*12*). Tetrodotoxin (TTX) blocked the bursts of action potentials but did not prevent the underlying oscillations of membrane potential (Fig. 1C); this result indicates that the potential oscillations underlying the bursts do not require Na^+ entry through TTX-sensitive channels and that burst firing probably does not involve local neuronal circuits within the tissue slice. Burst firing did not occur in Mg^{2+}-free solution, and it was not evoked by excitatory amino acids (kainate, quisqualate) that do not open Mg^{2+}-gated ion channels (*13*).

In other neurons, inward Ca^{2+} currents contribute to the onset of bursts of action potentials. Ca^{2+} current inactivation (*14*) or the development of an outward Ca^{2+}-dependent K^+ current (*15*) terminates the burst. However, burst firing of dopamine-containing cells persisted in Ca^{2+}-free solution ($n = 6$) (Fig. 1B), in apamin (1 μM), or with recording electrodes that contained the Ca^{2+} chelating agent 1,2-bis(2-aminophenoxy)ethane *N*,*N*,*N*′,*N*′-tetraacetic acid (BAPTA). BAPTA effectively buffered intracellular Ca^{2+} as demonstrated by blockade of the late component of the action potential after-hyperpolarization ($n = 5$) (*16*). Apamin, which blocks a Ca^{2+}-activated K^+ conductance in these (*17*) and other cells (*18*), actually increased the amplitude of the bursts, perhaps by blocking an opposing outward current during the depolarizing phase. Decreasing the K^+ concentration from 2.5 to 0.5 mM reversibly blocked burst firing ($n = 2$), and increasing the K^+ concentration to 10.5 mM increased the amplitude of the hyperpolarization between the bursts ($n = 2$). These findings are the opposite of those expected if the hyperpolarization had resulted from an increase in K^+ conductance.

Sodium was required for burst firing because, when its concentration was reduced (from 146 to 20 mM with choline or tris substitution), both the action potentials and the underlying membrane potential oscillations disappeared reversibly ($n = 3$) (Fig. 1D). One Na^+ current that has voltage and time dependence appropriate to burst firing is the hyperpolarization-activated current (I_h) (*19*). However, burst firing was not inhibited by Cs^+ (3 mM), which blocks I_h in dopamine-containing cells (*20*). We next hypothesized that Na^+ entry through NMDA-gated channels activated an electrogenic Na^+ pump. Both strophanthidin (2 to 10 μM, $n = 5$) and ouabain (2 to 10 μM) ($n = 6$) blocked burst firing in NMDA (Fig. 1E) but had little or no effect on the regular spike discharge observed in the absence of NMDA. Similar results were seen in the presence of dinitrophenol (30 to 100 μM) ($n = 5$) and in solutions without glucose ($n = 3$), both of which would be expected to inhibit active Na^+ extrusion.

Voltage-clamp experiments supported this hypothesis (*21*). The membrane was